Evolution of stripe and bubble domains in antiferromagnetically coupled $[(Co/Pt)_8/Co/Ru]_{18}$ multilayers

Cristina Bran,[1,2,*] Anna B. Butenko,[1,3] Nikolai S. Kiselev,[1,3] Ulrike Wolff,[1] Ludwig Schultz,[1] Olav Hellwig,[4] Ulrich K. Rößler,[1] Alexei N. Bogdanov,[1] and Volker Neu[1]

[1]*IFW Dresden, P.O. Box 270116, D-01171 Dresden, Germany*

[2]*IMPRS "Dynamical Processes in Atoms, Molecules and Solids," 01187 Dresden, Germany*

[3]*Donetsk Institute for Physics and Technology, 340114 Donetsk, Ukraine*

[4]*San Jose Research Center, Hitachi Global Storage Technologies, San Jose, California 95135, USA*

(Received 20 October 2008; revised manuscript received 16 December 2008; published 29 January 2009)

The magnetization process of antiferromagnetically coupled $[(Co/Pt)_8/Co/Ru]_{18}$ multilayers with perpendicular anisotropy is investigated via magnetic force microscopy at room temperature by imaging the domain configuration in magnetic fields. In the zero-field state, due to the perpendicular anisotropy, stripe domains characteristic for ferromagnetic coupling are observed. By increasing the external magnetic field, the domain configuration first modifies gradually, then transforms from continuous into isolated stripes, and changes in the end into bubbles, which collapse at higher fields. A theoretical model previously developed for bubble domains in single layer films is adapted for arbitrary complex multilayers and applied to the present layer architecture. The calculated values for strip-out and collapse fields compare well with the experimental results and demonstrate the validity of the theoretical description.

DOI: 10.1103/PhysRevB.79.024430 PACS number(s): 77.80.Dj, 75.70.Cn, 75.70.Kw, 68.37.Rt

I. INTRODUCTION

After the first observation of antiferromagnetic (AF) interlayer coupling between thin ferromagnetic (FM) layers via a metallic spacer layer[1,2] and its important application in electronic devices and magnetic recording technology,[3–5] extensive studies were performed on numerous combinations of magnetic and nonmagnetic layers but mostly with an in-plane anisotropy within the FM layer. In recent years, the study of the antiferromagnetic interlayer coupling has been extended to FM layers with perpendicular anisotropy,[6] which are of special interest for applications in perpendicular magnetic recording technology. One way of realizing such FM layers with perpendicular anisotropy is by utilizing the interface anisotropy of a very thin Co film, either as a single layer or within a multilayer consisting of Co and Pt or Pd.[7,8] In the well studied [Co/Pt]/Ru multilayer system,[9] which is composed of individual blocks of Co/Pt multilayers separated by thin Ru spacer layers, the balance of exchange coupling and dipolar coupling via the details of the multilayer architecture leads to a large variety of different magnetic zero-field states, which are observed using domain imaging techniques.

In the homogeneous AF state, the magnetization is laterally correlated in each individual Co/Pt block but antiparallel from block to block in order to minimize the AF interlayer coupling. In the FM stripe domain state, the perpendicular magnetization is correlated in vertical direction throughout the whole block but forms neighboring domains with opposite magnetization direction in order to minimize the stray field energy. A third magnetic phase, the so-called AF stripe state is expected to exist for large AF exchange but has not been realized experimentally so far. Stray field calculations in combination with magnetic force microscopy (MFM) contrast simulations, however, suggest that such domains should be resolvable by high-resolution MFM when they are present.[10] Consequently, the detailed study of domain structure and magnetization processes, and their description by domain theory is an important contribution to quantitatively describe the complex interactions present in these multilayers. In this paper, we study the domain structure and the magnetization processes in a rather thick [Co/Pt]/Ru multilayer, which zero-field state is characterized by the above described FM stripe domains also common for simple single layer films with perpendicular anisotropy. Strictly speaking, the AF coupling violates the stripe coherency through the stack, inducing a relative transverse shift of domains in the adjacent layers.[11] However, for multilayers with the FM stripe ground state (as in this paper), this shift is very small and is not considered. In-field MFM measurements are performed to follow the evolution of the domain structure in a perpendicular oriented magnetic field in the ascending and descending branches of the first quadrant of magnetization curve. The qualitative similarity of the behavior to that of bubble domains known in single layer films[12] and multilayers without antiferromagnetic spacer layer[13,14] suggests a possible description of the observed phenomena in these multilayers by a modified bubble theory. Thus, after describing the experimental details, the results of the paper are organized in three sections. Section III deals with the experimental observations by in-field MFM and global magnetometry. The following section develops a modified bubble theory, which treats the stray field energy terms in a rigorous approach including all internal magnetic charges of the multilayer stack (Sec. IV), and a final section (Sec. V) compares quantitatively the experimental results with the modified theory for the multilayer architecture investigated in this study.

II. EXPERIMENTAL PROCEDURES

The multilayer system used for our experiments is $\{[Co(0.4\ nm)/Pt(0.7\ nm)]_8Co(0.4\ nm)/Ru(0.9\ nm)\}_{18}$,

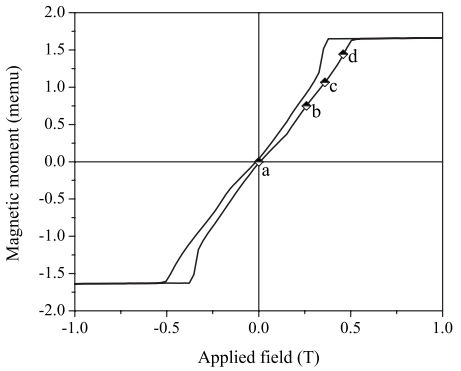

FIG. 1. (a) Schematic view of the MFM setup and (b) magnetic field H_z measured in lateral displacement, at different distances from the sample: (i) 1.2, (ii) 1.4, (iii) 2, (iv) 2.5, (v) 3, (vi) 4, (vii) 6, and (viii) 11 mm.

which is in the following referred to as the [Co/Pt]/Ru multilayer. The sample was deposited by magnetron sputtering (3 mTorr Ar pressure) at ambient temperature onto Si_3N_x coated Si substrates with a 20 nm Pt seed layer and a 2 nm Pt cap for oxidation protection. Details on sample preparation are given in Ref. 15. The sample was structured in isolated square shaped elements with lateral size of 12 μm using optical lithography. This way, it is easier to compare the position of subsequent measurements and furthermore the scan across the nonmagnetic area can be used as a correction for a possible offset in the phase shift of the MFM experiment.

Magnetic hysteresis at room temperature with field perpendicular to the film plane was measured using a quantum design physical properties measurement system (PPMS) with vibrating-sample magnetometer (VSM) in a maximum field of 3 T. The local magnetization distribution was studied using a digital instrument dimension 3100 atomic force microscope with MFM extender box for phase-shift measurements. The topography scan was performed in tapping mode and the magnetic contrast was measured in an interleave scan with a lift height of 50 nm. Standard magnetic tips (MESP, Veeco) were magnetized along the tip axis prior to the MFM measurements.

In order to apply a perpendicular magnetic field to the sample during MFM measurements, a strong pyramidal stack of NdFeB permanent magnets with their texture axis perpendicular to the sample surface was lifted gradually to approach the sample from below. The full sample size (<3 mm) is typically smaller than the smallest dimensions of the magnet. The sample is placed with precision of ± 0.5 mm above the center of the magnet, guaranteeing a perpendicular orientation of the field in the sample center [Fig. 1(a)]. The field distribution above the permanent magnet was measured with a Mag-Scan Hall-probe system. The lateral field homogeneity is better than 1% within a radius of 1 mm from the center of the magnet, and the field strength in the central area can be varied from 0.02 T up to a maximum of 0.6 T for a fully approached magnet[16] [Fig. 1(b)].

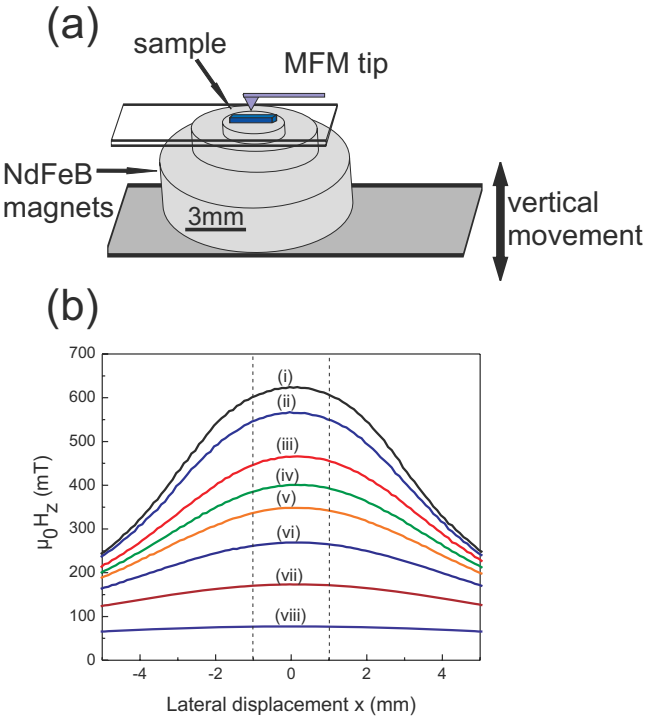

FIG. 2. (Color online) Hysteresis loop of [Co/Pt/]/Ru multilayer measured by VSM with field perpendicular to the sample surface. The points represent the field values used for the MFM measurements presented in Fig. 4.

III. IN-FIELD DOMAIN OBSERVATION

Figure 2 shows the magnetization curve of the [Co/Pt]/Ru multilayer as a function of the applied field, which is oriented perpendicular to the film plane. At zero applied field the film is in a nearly demagnetized state with a remanence close to zero. By increasing the field value, the magnetization increases almost linearly until it reaches saturation. At this point, the film is completely magnetized in the direction of the applied field. Reducing the field from positive saturation, the magnetization curve shows a kink in the first quadrant, and, after that, abruptly reduces and continues to decrease with decreasing field. As the film is always parallel to the anisotropy axis, rotational processes are not expected in the magnetization reversal; thus the reversal may happen via nucleation of reversed domains and their expansion until at large negative field the former positive domains are fully expelled from the film.

From these out-of-plane measurements we extract the value for saturation polarization $4\pi M_s = 0.765$ T and the coercive field $\mu_0 H_c = 0.01$ T. Shown in Fig. 3 are MFM images of the sample taken in three different remanent states. The dark and bright contrast corresponds to domains with magnetization pointing out and into the plane of the film, respectively. In the as-prepared state [Fig. 3(a)], the image is characterized by a labyrinth stripe domain pattern. After out-of-plane saturation, the multilayers exhibit a random maze domain pattern as shown in the MFM image in Fig. 3(b). The average domain width in both cases is about 180 nm. Applying a saturating in-plane magnetic field with subsequent in-

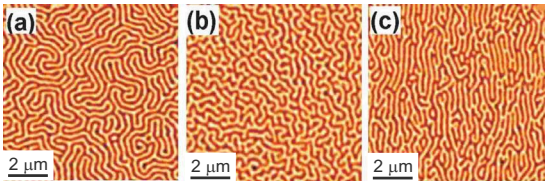

FIG. 3. (Color online) MFM images of [Co/Pt]/Ru in three different remanent states: (a) in as-prepared state, (b) after out-of-plane saturation, and (c) after ac demagnetizing in plane.

plane ac demagnetization changes significantly the domain pattern, and also the average domain width is reduced to about 135 nm. The in-plane magnetic field couples to the in-plane magnetization component of the domain wall and aligns the stripe domains parallel to the external field direction as it is visible in Fig. 3(c).[17] Numerical calculations of dipolar sums predict that the parallel stripes are energetically favored over a labyrinth domain or maze domain structure [Figs. 3(a) and 3(b)].[18] Above comparison, however, shows that the domain configuration in the remanent state depends strongly on the magnetic history, and the energetically lowest state has to be initiated by an appropriate demagnetizing procedure.

Figure 4 shows a series of MFM images for different magnetic fields applied perpendicular to the sample during measurement. As explained in Sec. II, the film was structured for an easier recognition of the scanned area. The equilibrium domain width of the structured sample is comparable to that of the extended film shown in Fig. 3(a). For the given structure geometry and size, we thus do not observe any influence of the lateral confinement on the domain configuration. For smaller structures this cannot be excluded and presents an interesting topic for future studies. Starting from the demagnetizing state, in fields which are small compared to the saturation field, the domains change very slowly. The first magnetizing process can be observed at the rim of the element where bright domains oriented parallel to element edge disappear first. This can be understood from the unfavorably large magnetostatic energy for such oriented domains due to large stray fields.[19] By increasing the external magnetic field, the domains which are aligned parallel to the

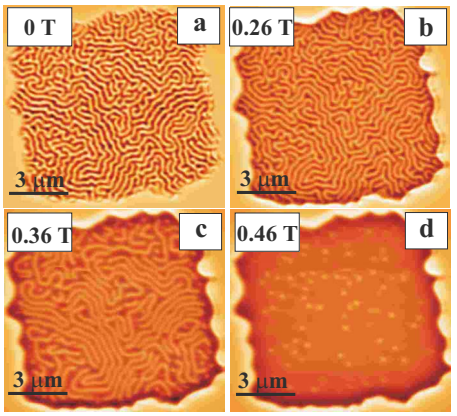

FIG. 4. (Color online) Domain structures of [Co/Pt]/Ru multilayer recorded along the increasing branch of the hysteresis.

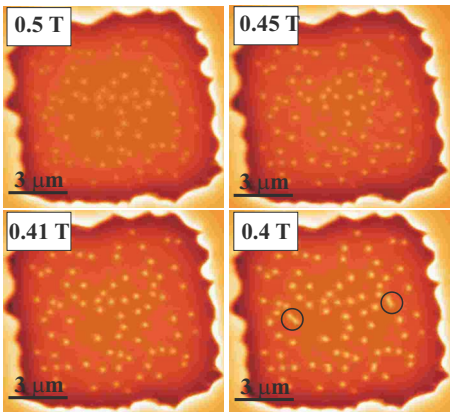

FIG. 5. (Color online) Sequence of MFM images recorded on the decreasing branch of a minor loop.

field grow while the oppositely aligned domains get smaller. This process occurs gradually until the domains transform into isolated stripes and, in the end, into a bubble domain structure at higher fields. However, near the strip-out instability field (the field in which the elongated domains with opposite magnetization transform into bubble domains), a rapid growth of the preferably aligned domains can be observed. During this process, the width of the domains oriented opposite to the applied field remains nearly constant while they contract along their lengths.[20] As the external field is increased, the domains contract so that only bubbles exist at magnetic fields greater than the strip-out field. Further increase in the external field causes the bubbles to shrink until, at a critical field (collapse field) of 0.52 T, they collapse (not shown here).

In order to obtain a more precise quantitative field value at which the strip-out instability occurs, a series of MFM images was recorded now on the decreasing branch of a minor loop in a narrow field range close to saturation (Fig. 5). By this we can ensure that the strip out starts from isolated bubbles and is not influenced by the domain configuration at lower fields. Starting from highest value where the bubbles still exist (0.5 T), upon decreasing the field the bubble shape and configuration stay stable but the MFM contrast arising from the bubbles changes gradually down to 0.41 T. This is best seen in exemplary MFM profiles extracted from the measurements across an individual isolated bubble as a function of the applied field (Fig. 6).

Both the full width at half maximum and the absolute MFM contrast increase with decreasing field, which is inter-

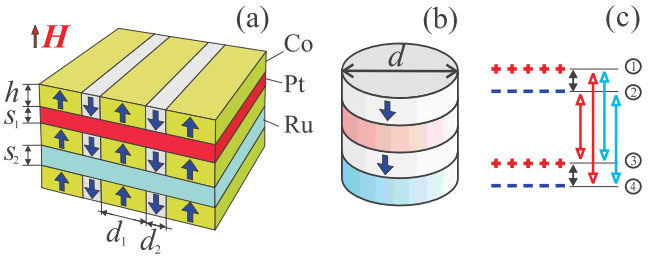

FIG. 6. (Color online) MFM profile of an isolated bubble for different applied fields.

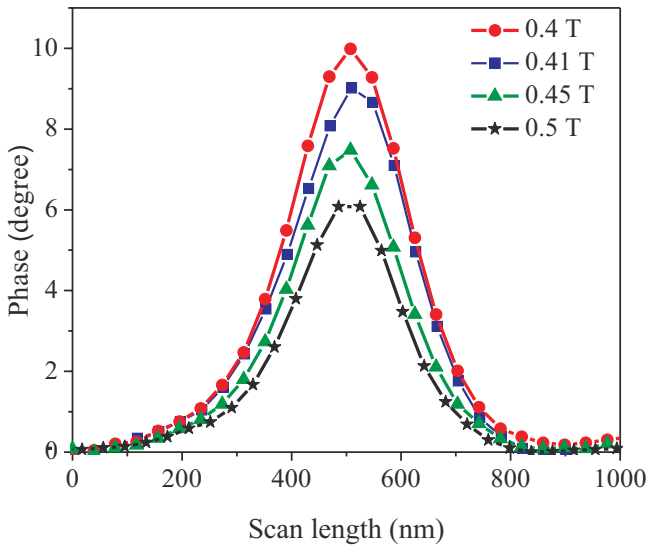

FIG. 7. (Color online) (a) A fragment of a multilayer with stripe domains, (b) an isolated bubble, and (c) contributions of the magnetostatic interaction between two layers.

preted as a continuous enlargement of the bubble. As described in Sec. II, MFM records only the force gradient experienced by a magnetic tip due to the magnetostatic interaction with the z component of the bubble stray field. The contrast is thus also largely dependent on the magnetic structure and the volume of the tip coating, and is necessarily broadened compared to the true size of the bubble. Thus, we cannot conclude on the exact bubble diameter from our MFM measurements with an uncalibrated tip.

IV. MICROMAGNETIC MODEL

To explain the experimental results presented above, an appropriate domain model for coupled multilayers is derived in the following. Micromagnetic theory of multilayers with stripe and bubble domains have been developed quite some time ago[21–23] and have been applied for numerical calculations of multidomain patterns in a number of practical cases.[22,23] Contrary to systems investigated in Refs. 22 and 23 in modern superlattices with perpendicular anisotropy ([Co/Pt] and others), the equilibrium sizes of domains strongly exceed the magnetic layer thickness.[24] For such structures the calculations become arduous due to slow convergence of infinite sums in the stray field energy. In this section we execute integral transformations of the dipolar magnetostatic energy and derive effective micromagnetic equations to calculate the existence regions and geometrical parameters of equilibrium stripe domains and their evolution in a bias field.

We consider a superlattice consisting of $N^*=NX$ identical magnetic layers with the magnetization M and thickness h separated by spacer layers of thickness s_i [see Fig. 7(a)]. Furthermore, for every X magnetic layers, the separating spacer layer is assumed to mediate an antiferromagnetic coupling. Such a model allows describing multilayers with different spacer thickness. In particular, for $[(\mathrm{Co/Pt})_{X-1}/\mathrm{Co/Ru}]_N$ multilayers

$$s_i = \begin{cases} s_{\mathrm{Ru}} = 0.9 \text{ nm} & \text{for } i = mX, \ m = 1 \ldots N \\ s_{\mathrm{Pt}} = 0.7 \text{ nm} & \text{other} \end{cases}$$

and $h=h_{\mathrm{Co}}=0.4$ nm [Eq. (7)]. Generalizing the results of Refs. 10, 11, and 25, we can write the energy density of the stripe phase (per one layer) in the following form:

$$w_s = 8\pi M^2 \frac{l_c}{D} + \frac{J}{h}\left(1 - \frac{1}{N}\right) - HMq + 2\pi M^2 \tilde{N}(D,q), \quad (1)$$

where $D=d_1+d_2$ is the stripe period, $q=(d_1-d_2)/D$ is the domain imbalance, $J>1$ is the antiferromagnetic exchange interaction coupling constant, and $l_c=\sigma/4\pi M^2$ is the characteristic length, defined by the ratio of wall energy density σ and the magnetostatic energy density $2\pi M^2$. The first term in Eq. (1) describes the wall energy density of the FM stripe domain pattern and the second term quantifies the antiferromagnetic exchange energy, which has to be paid at all $N-1$ Ru containing interfaces. The third term (Zeeman term) lowers the energy when domains grow with magnetization parallel to the field. The remaining stray field energy density is expressed with the help of an effective demagnetizing factor:

$$\tilde{N}(D,q) = \underbrace{1 - \Omega_s(h)}_{w_{m0}^{(s)}} + w_m^{(s)}(D,q), \quad (2)$$

which includes the self-energy of individual magnetic layers ($w_{m0}^{(s)}$) and the interaction between them ($w_m^{(s)}$).

$$\Omega_s(\omega) = \frac{4\omega^2}{\pi h D}\int_0^1 (1-t)\ln\left[1 + \frac{\cos^2(\pi q/2)}{\sinh^2(\pi\omega t/D)}\right]dt, \quad (3)$$

$$w_m^{(s)}(D,q) = -\frac{1}{N^*}\sum_{k=1}^{N^*-1}\sum_{n=k+1}^{N^*}\Xi_s(L_{nk}), \quad (4)$$

where

$$\Xi_s(L_{nk}) = 2\Omega_s(L_{nk}) - \Omega_s(L_{nk}-h) - \Omega_s(L_{nk}+h) \quad (5)$$

is equal to the stray field coupling energy between two layers separated by distance

$$L_{nk} = h(n-k) + \sum_{i=k}^{n-1} s_i. \quad (6)$$

The factors $\Xi_s(L_{nk})$ [Eq. (5)] are composed of the four contributions of the dipolar magnetostatic interactions between pairs of the "charged" planes bounding the layers [Fig. 7(c)], namely, interactions between like charges $1\leftrightarrow 3$ and $2\leftrightarrow 4$ yield equal (positive) energy contributions $\Omega_s(L_{nk})$ while $1\leftrightarrow 4$ and $2\leftrightarrow 3$ couplings yield negative-energy contributions, $\Omega_s(L_{nk}+h)$ and $\Omega_s(L_{nk}-h)$, correspondingly. Summation over all the layer pairs yields the interaction energy [Eq. (4)] (see details of the method in Refs. 10, 11, and 25).

As already indicated in Sec. I, the AF coupling influences the details of the FM stripes by inducing a relative shift in the adjacent layers which can be estimated for the present multilayers as $a=CJ/(2\pi M^2)$ to be less than 2 nm (where C is certain function of multilayer geometrical parameters, $J=0.46$ erg/cm^2 and $2\pi M^2=2.3$

$\times 10^6$ erg/cm^3).[11] In multilayers with the AF ground-state (e.g., $\{[\mathrm{Co}(0.4\ \mathrm{nm})/\mathrm{P}(0.7\ \mathrm{nm})]_{X-1}/\mathrm{Co}(0.4\ \mathrm{nm})/\mathrm{Ru}(0.9\ \mathrm{nm})\}_N$ superlattices with $N=18$ and $X \leq 8$), the exchange shift is a sizable effect and causes a lateral instability of metastable FM stripes at certain critical thickness.[11] Furthermore, in these systems the interplay between the antiferromagnetic coupling and the demagnetization forces leads to the formation of specific topological defects and a magnetic-field-induced sequential switching of the different Co/Pt blocks (so-called *metamagnetic* transitions).[9,26]

Considering now an isolated bubble of diameter d [Fig. 7(b)], the energy in the multilayer can also be written as a sum of wall energy, Zeeman energy, and magnetostatic energy:

$$w_b = 4\pi^2 M^2 N^* \left(l_c h d + \frac{Hhd^2}{8\pi M} + \frac{2d^3}{3\pi} - \Omega_b(h) + w_m^{(b)} \right). \quad (7)$$

The antiferromagnetic exchange only adds a constant term independent of the bubble geometry and is not considered. Again, the magnetostatic energy can be expressed as the self-energy of an individual magnetic disk plus the sum of the dipolar interaction between different magnetic disks:

$$w_m^{(b)} = -\frac{1}{N^*} \sum_{k=1}^{N^*-1} \sum_{n=k+1}^{N^*} \Xi_b(L_{nk}), \quad (8)$$

$$\Xi_b(L_{nk}) = 2\Omega_b(L_{nk}) - \Omega_b(L_{nk}-h) - \Omega_b(L_{nk}+h), \quad (9)$$

$$\Omega_b(\omega) = -\frac{2d}{3\pi u}[(\omega^2 - d^2)E(u) - \omega^2 K(u)], \quad (10)$$

where $K(u)$ and $E(u)$ are the complete elliptical integrals as defined in Ref. 27, $u = d/\sqrt{\omega^2 + d^2}$.

Particularly, for equal spacer thickness $s_i = s$, the interaction energies [Eqs. (4) and (8)] can be simplified,

$$w_m^{(s),(b)} = -\frac{1}{N^*} \sum_{k=1}^{N^*-1} (N^* - k)\Xi_{s,b}(Tk), \quad (11)$$

where $T = h + s$ is the period of the multilayer.

The equilibrium parameters of the stripes are derived by minimization of energy w_s [Eq. (1)] with respect to D and q, and minimization of Eq. (7) yields the equilibrium bubble diameter. In particular, for multilayers with equal spacers, the latter is derived from the following equation:

$$l_c h + \frac{Hhd}{4\pi M} - F(d) = 0, \quad (12)$$

where

$$F(d) = \frac{2d}{\pi}\left\{ -d + f(h) - \sum_{k=1}^{N^*-1} \left(1 - \frac{k}{N^*}\right)\Xi_f(Tk) \right\},$$

$$\Xi_f = 2f(Tk) - f(Tk+h) - f(Tk-h),$$

$$f(\omega) = \sqrt{\omega^2 + d^2}E(u). \quad (13)$$

V. COMPARISON BETWEEN THEORETICAL MODEL AND EXPERIMENTAL RESULTS

The observed magnetization processes resemble those seen in single layer thick films with perpendicular anisotropy.[12] Close to saturation, the labyrinth stripe domains contract to form isolated stripe domains and transform further into bubble domains. The bubble domains transform into elongated stripes at H_{bs} and collapse at a critical field H_{bc}.

The calculations of the equilibrium parameters in [Co/Pt]/Ru have been carried out with the characteristic length $l_c = 4.43$ nm. This value has been derived from analysis of the domain periods measured in series of $[\mathrm{Co}(0.4\ \mathrm{nm})/\mathrm{Pt}(0.7\ \mathrm{nm})]_X$ multilayers.[14]

At zero-field minimization of energy (1) yields the solution $D_0 = 264.3$ nm for stripe period, which is very close to the observed stripe period after in-plane ac demagnetization [270 nm, Fig. 3(c)].

It is well known that the existence of solitary bubbles is restricted by strip-out instability at lower fields and a collapse at high fields.[27] A similar situation occurs for bubbles in multilayers. Following the standard methods (see, e.g., Ref. 27), one can derive the critical parameters of the bubble existence based on two stability criteria. The equation $S_{bc} = l_c$ defines the critical minimum diameter (collapse diameter) d_{bc} down to which an isolated bubble is stable for a film with given architecture and materials properties (l_c). Furthermore, the analysis of elliptical distortion results in an upper critical diameter d_{bc}, defined by $S_{bs} = l_c$, above which a cylindrical bubble will elongate and transform into a stripe (strip-out diameter). The two stability functions are given as

$$S_{bc}(d) = \frac{2d}{\pi h}\left[d + f_{bc}(h) - \sum_{k=1}^{N^*-1} \left(1 - \frac{k}{N^*}\right)\Xi_{bc}(Tk) \right], \quad (14)$$

$$\Xi_{bc}(Tk) = 2f_{bc}(Tk) - f_{bc}(Tk+h) - f_{bc}(Tk-h),$$

$$f_{bc}(\omega) = -\sqrt{\omega^2 + d^2}E(u) + \frac{\omega^2}{\sqrt{\omega^2 + d^2}}K(u), \quad (15)$$

and

$$S_{bs}(d) = -\frac{1}{3}\left(S_{bc}(d) + \frac{d^2}{2\pi h}F_{bs}(d) \right), \quad (16)$$

$$F_{bs}(d) = \frac{16}{3}\left[f_{bs}(h) - 1 - \sum_{k=1}^{N^*-1} \left(1 - \frac{1}{N^*}\right)\Xi_{bs}(Tk) \right], \quad (17)$$

$$\Xi_{bs}(Tk) = 2f_{bs}(Tk) - f_{bs}(Tk+h) - f_{bs}(Tk-h),$$

$$f_{bs} = \frac{\sqrt{\omega^2 + d^2}}{d^3}\{(2\omega^2 + d^2)E(u) - 2\omega^2 K(u)\}. \quad (18)$$

Within the limits given by d_{bc} and d_{bs}, a cylindrical bubble is stable and its size is an unambiguous function of

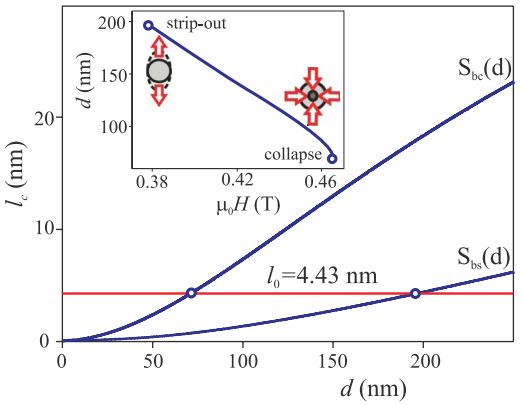

FIG. 8. (Color online) The characteristic functions $S_{bc}(d)$ and $S_{bs}(d)$ determine bubble sizes at collapse (d_{bc}) and strip-out (d_{bs}) fields. For [Co/Pt]/Ru multilayer (l_c=4.43 nm), we obtained d_{bc} =69.76 nm and d_{bs}=193.47 nm. The inset shows the equilibrium values of the bubble diameters as a function of the bias field.

the external field according to Eq. (12). For the studied multilayer with X=9 and N=18, the stability functions are given in Fig. 8 in dependence of the diameter d and their intersection with l_c results in strip-out and collapse diameters. The inset shows the variation in d within the stability region as a function of the applied field.

For the present [Co/Pt]/Ru multilayers we estimate $\mu_0 H_{bs}$=0.38 T and $\mu_0 H_{bc}$=0.47 T, which are values in good agreement with the experimental ones $\mu_0 H_{bs,\mathrm{exp}}$ =0.4 T and $\mu_0 H_{bc,\mathrm{exp}}$=0.52 T.

VI. CONCLUSION

In conclusion, we have investigated the magnetization processes of AF-coupled [Co/Pt]/Ru with perpendicular anisotropy by direct MFM observation. The magnetization proceeds as typical for single layer thin films with perpendicular anisotropy via gradual growing of the domains oriented in the same direction with the applied field and contracting of those oriented opposite to the applied field. Strip-out and collapse fields have been determined from domain imaging in narrow subsequent field steps. A micromagnetic theory which treats stripe and bubble domains in multilayer films with small individual layer thicknesses has been developed and applied to the experimentally studied multilayer architecture.

With only one free parameter, the characteristic length l_c, which was determined to 4.43 nm, the theory can describe the equilibrium domain width of the sample in the ac demagnetized state, and the strip-out and collapse fields of the bubble domains with very good precision. Combining this theory with domain observation thus helps in deducing the physical properties such as wall energy and coupling interaction in complex magnetic multilayers.

ACKNOWLEDGMENTS

Lithographic structuring by I. Mönch and S. Sieber is gratefully acknowledged. A.B.B., N.S.K., and U.K.R. thank DFG for support through SPP1239 project A8. A.B.B., N.S.K., and A.N.B. thank H. Eschrig for support and hospitality at the IFW Dresden.

*Corresponding author; c.bran@ifw-dresden.de

[1] P. Grünberg, R. Schreiber, Y. Pang, M. B. Brodsky, and H. Sowers, Phys. Rev. Lett. **57**, 2442 (1986).
[2] M. N. Baibich, J. M. Broto, A. Fert, F. Nguyen Van Dau, F. Petroff, P. Etienne, G. Creuzet, A. Friederich, and J. Chazelas, Phys. Rev. Lett. **61**, 2472 (1988).
[3] C. Chappert, H. Bernas, J. Ferre, V. Kottler, J. P. Jamet, Y. Chen, E. Cambril, T. Devolder, F. Rousseaux, V. Mathet, and H. Launois, Science **280**, 1919 (1998).
[4] T. Thomson, G. Hu, and B. D. Terris, Phys. Rev. Lett. **96**, 257204 (2006).
[5] B. Rodmacq, V. Baltz, and B. Dieny, Phys. Rev. B **73**, 092405 (2006).
[6] O. Hellwig, T. L. Kirk, J. B. Kortright, A. Berger, and E. E. Fullerton, Nature Mater. **2**, 112 (2003).
[7] P. F. Carcia, A. D. Meinhaldt, and A. Suna, Appl. Phys. Lett. **47**, 178 (1985).
[8] S. Hashimoto, Y. Ochiai, and K. Aso, J. Appl. Phys. **66**, 4909 (1989).
[9] O. Hellwig, A. Berger, J. B. Kortright, and E. E. Fullerton, J. Magn. Magn. Mater. **319**, 13 (2007).
[10] N. S. Kiselev, I. E. Dragunov, V. Neu, U. K. Rößler, and A. N. Bogdanov, J. Appl. Phys. **103**, 043907 (2008).
[11] N. S. Kiselev, I. E. Dragunov, U. K. Rößler, and A. N. Bogdanov, Appl. Phys. Lett. **91**, 132507 (2007).
[12] A. A. Thiele, J. Appl. Phys. **41**, 1139 (1970).
[13] A. W. Rushforth, P. C. Main, and B. L. Gallagher, J. Appl. Phys. **89**, 7534 (2001).
[14] J. E. Davies, O. Hellwig, E. E. Fullerton, G. Denbeaux, J. B. Kortright, and K. Liu, Phys. Rev. B **70**, 224434 (2004).
[15] O. Hellwig, A. Berger, and E. E. Fullerton, Phys. Rev. B **75**, 134416 (2007).
[16] The closest distance of 1.2 mm is given by the thickness of sample platform and substrate.
[17] A. Hubert and R. Schäfer, *Magnetic Domains* (Springer-Verlag, Berlin, 1998).
[18] M. Pardavi-Horvath, J. Oti, G. Vertesy, L. H. Bennett, and L. J. Swartzendruber, J. Magn. Magn. Mater. **104-107**, 313 (1992).
[19] V. Neu, S. Melcher, U. Hannemann, S. Fähler, and L. Schultz, Phys. Rev. B **70**, 144418 (2004).
[20] Th. Eimüller, R. Kalchgruber, P. Fischer, G. Schütz, P. Guttmann, G. Schmahl, M. Köhler, K. Prügl, M. Scholz, F. Bammes, and G. Bayreuther, J. Appl. Phys. **87**, 6478 (2000).
[21] A. Suna, J. Appl. Phys. **59**, 313 (1986).
[22] H. J. G. Draaisma and W. J. M. de Jonge, J. Appl. Phys. **62**, 3318 (1987).
[23] S. Honda, Y. Ikegawa, and T. Kusuda, J. Magn. Magn. Mater. **111**, 273 (1992).

[24] U. K. Rößler and A. N. Bogdanov, J. Magn. Magn. Mater. **269**, L287 (2004).
[25] A. N. Bogdanov and D. A. Yablonskii, Fiz. Tverd. Tela (Leningrad) **22**, 680 (1980) [Sov. Phys. Solid State **22**, 399 (1980)].
[26] N. S. Kiselev, U. K. Rößler, A. N. Bogdanov, and O. Hellwig, Appl. Phys. Lett. **93**, 162502 (2008).
[27] A. Hubert and R. Schäfer, *Magnetic Domains* (Springer Verlag, Berlin, 1998), p. 313.